Measurement 145 (2019) 178–189

Contents lists available at ScienceDirect

Measurement

journal homepage: www.elsevier.com/locate/measurement

Research on the milling tool wear and life prediction by establishing an integrated predictive model

Yinfei Yang [1], Yuelong Guo [1], Zhiping Huang, Ni Chen *, Liang Li, Yifan Jiang, Ning He

National Key Laboratory of Science and Technology on Helicopter Transmission, Nanjing University of Aeronautics and Astronautics, Nanjing 210016, China

ARTICLE INFO

Article history:
Received 2 March 2019
Received in revised form 1 May 2019
Accepted 6 May 2019
Available online 10 May 2019

Keywords:
Tool wear
Remaining useful life
Integrated prediction model
Trajectory similarity
Support vector regression

ABSTRACT

As the tool wear increases, the surface quality of the workpiece will decrease, and even the workpiece will be scrapped. Therefore, in order to obtain a better machined workpiece quality, monitoring the tool wear is necessary. By monitoring the machining condition, the degree of the tool wear and the remaining useful life (RUL) can be obtained in time. This paper establishes an integrated prediction model based on trajectory similarity and support vector regression, which can predict the tool wear and life. The time domain and wavelet analysis are carried out. The relationship between the signal characteristic quantity and the tool wear is studied. Five eigenvectors are selected as the input vectors of the prediction model by studying the correlation between 45 characteristic quantities and the tool wear. The model training is carried out by using the PHM public data set. The relative errors of VB value prediction accuracy in the stable stage of the sample tool is above 88% and the prediction accuracy of the stable stage of Tool 1, 2, and 3 is 88.5%, 87.5%, and 90.5% respectively, by using this integrated prediction model, which is better than other four single algorithms.

1. Introduction

At present, the tool wear is always determined through two methods: manual experience and supplier recommendations [1]. In general, as the tool wears, many factors will change, including the vibration generated by the machine tool, the sound produced in cutting process, the chip shape, the machine power and so on [2–4]. Experienced operators can determine if the tool has failed according to these changes. This way is easy to cause two problems: Firstly, it's too early to change the tool that the tool has not reached the service life, which causes tool waste and increases tool cost; Secondly, if the tool changes too late, it is easy to cause that the surface precision of the parts is not enough or the parts are damaged because the tool is working in a failure state [5–7]. Especially in the aerospace field, the cost will be very high, which will seriously affect the production efficiency and economic benefits of the enterprise. Therefore, accurate prediction of the tool life is much important to manufacturing companies. Some statistical studies have shown that a reasonable tool change time and strategy can effectively reduce downtime by 75%, increase production efficiency by 10%-60%, and reduce production costs by 10%–40% [8].

Some researchers have done works about methods that reducing tool wear to improve machining economy and analyzing surface roughness and chip morphology in different machining conditions. Dhar et al. [9] used minimum quantity lubrication (MQL) in turning AISI-4340steel, which reducing tool wear and improving surface roughness. Maruda et al. [10] presented minimum quantity cooling lubrication with extreme pressure and anti-wear (MQCL + EP/AW) method and compared surface topographies obtaining after turning for dry, MQCL and MQCL + EP/AW. The result showed that MQCL + EP/AW could get the best surface topography parameters. Twardowski et al. [11] found that the dominant factor influencing surface roughness in end milling of hardened steel in high speed milling (HSM) was dynamical phenomena and feed per revolution. De Aguiar et al. [12] achieved that using long tools with long lives and small diameters to get good surface roughness. Wojciechowski and Mrozek [13] optimized micro ball end milling tool's axis slope along the toolpath and feed per tooth and reduced vibration and improved surface roughness. Zhang et al. [14] revealed that tool flank wear could truncate the chips at both cut-in and cut-out slides and reduce the length of chips in the feed direction in ultra-precision machining. Wojciechowski et al. [15] found that the mechanisms of surface

* Corresponding author.
E-mail address: ni.chen@nuaa.edu.cn (N. Chen).
[1] These authors contributed equally to this work and should be considered co-first authors.

https://doi.org/10.1016/j.measurement.2019.05.009
0263-2241/

roughness was mainly affected by the value of tool's overhang during finishing ball end milling.

Many Researchers are actively seeking effective methods to monitor the tool wear and RUL in time. However, these methods are still in the development stage, and their reliability and adaptability are still difficult to meet the actual situation. They have become an major technical obstacle for automated and intelligent production. In recent years, with the development of the modern sensing technology, the signal processing technology (such as wavelet, fractal, hybrid, time–frequency analysis, etc.) and the rapid development of pattern recognition technology (such as fuzzy logic, neural networks, support vector machine, expert system, etc.), it is valuable to study how to apply these advanced technologies to the tool condition monitoring system to enhance the system reliability and versatility.

The tool wear and RUL prediction are needed to be carried out according to the following steps: collecting specific sensor signals, then selecting appropriate methods to process the signals, extract characteristic parameters sensitive to the tool wear, and finally establishing predictive model. The relationship between the characteristic quantity and the tool wear is not linear in the cutting process. In machining process, the cutting force can well reflect the state of the tool. The tool wear will occur in different degrees when machining parts. Force signals are collected by the corresponding force measuring device, and the current state of the tool is evaluated after analysis [16]. Then the RUL of the tool is obtained according to the law of the tool wear.

The milling tool contacts intermittently with the workpiece. It is not feasible to evaluate the state of the tool directly by the magnitude and variation of the cutting force [17]. Researchers always study the characteristic quantities of the force signal in time domain, frequency domain or time-frequency domain [18]. Therefore, the accurate prediction of the RUL of tool can only be made by analyzing the signals and choosing appropriate characteristic quantities. Sohyung et al. [19] selected the maximum the cutting force as the characteristic quantity, and used the support vector machine for pattern recognition training to predict the RUL of the tool. Letot et al. [20] used four signals to predict the RUL of the tool, including cutting force, vibration, sound, and machine power under the same model, and found that the analysis based on force signal was the best. Jáuregui et al. [21] determined the state of wear of the tool through analyzing the force and vibration signal during machining. They found that the prediction results of the force signal were better than that of the vibration signal. Dong et al. [22] collected the force signal during the machining process and 16 sets of eigenvalues were extracted from it, then predicted the tool wear by using the neural networks model and achieved ideal results. Azmi [23] collected the cutting force data during the machining glass fiber reinforced polymer (GFRP) composites process, and proposed a new tool condition monitoring method using these data. The results showed that this method had good predictability for the state of the tool wear. Nouri et al. [24] proposed that the real-time acquisition of the tool wear could be feasible through monitoring the coefficients of the force model. They normalized the tangential force and radial force model coefficients, then combined the two parameters into one coefficient for the tool wear monitoring.

At present, artificial intelligence technology is widely applied to monitoring the tool wear and life. Especially, neural networks and its various derivative models are widely used [25–29]. At the same time, the support vector machine (SVM) also has more applications. Xu et al. [30] collected the data of the CNC system directly, then monitored the state of the tool breakage by incremental cost-sensitive support vector machine (ICSSVM) technology. The results showed that the technology was stable and reliable. Shi and Gindy [31] collected multiple signals in the machining process and processed signal by the principal component analysis (PCA) technique and established the least squares SVM (LS-SVM) model to obtain a better results. Yu et al. [32] proposed a weighted hidden Markov model (HMM) to describe dynamic characteristics of the tool wear law, and then established the probability prediction method including this model, and obtained good experimental results. Niaki et al. [33] used the extended Kalman filter (EKF) to monitor the tool wear when machining workpiece under various feed speed conditions. It could effectively improve the estimation accuracy than other deterministic methods for estimating the wear area of the tool. Zhang et al. [34] established a probability model including Particle Learning (PL). This model could effectively avoid the complexity of modeling for the specific tool wear, which had good robustness and saved computation time. Penedo et al. [35] established a comprehensive method using the least squares regression technique and fuzzy *k*-nearest-neighbors (K-NN) technique to monitor the state of the tool wear. Compared with the traditional inductive fuzzy neural model, this method has better performance.

Although neural networks are widely used, there are some problems with it. On the one hand, it is difficult to deal with the problem that the network scale is not coordinated with the actual scale. On the other hand, due to that the initial weight of the neural networks has many initialization methods, different methods will cause different results. In addition, the threshold of the training process and training sample data are different, so the result will be seriously deviated and the stability of the algorithm is not high in the prediction. Support vector regression (SVR) is a generalized model of SVM. It utilizes the idea of infinite approximation, and can achieve optimal solutions with little historical data, and has strong promotion ability. The application of the kernel function reduces the complexity of the model and can be widely applied to nonlinear regression prediction. However, SVR also has shortcomings. For example, the initial parameters are needed to be manually set, and the workload is large, which is easy to cause low accuracy of the prediction.

This paper establishes an integrated prediction model based on the trajectory similarity based prediction (TSBP) and the differential evolution SVR (DE-SVR) algorithm. The tool wear and RUL can be predicted by the TSBP algorithm according to the variation law of the signal characteristic quantity in the milling process. The optimal solution can be realized by the DE-SVR algorithm according to the limited data amount, which could improve the model prediction accuracy, and solve the problem of complicated parameter setting. The force signal is collected during the cutting process, and the time-domain, frequency-domain and wavelet analysis are performed. The most representative characteristic quantity is extracted, and the characteristic vector is imported into the integrated model for prediction. The predicted value is compared with the actual value. At the same time, the integrated model is compared with other models in prediction accuracy.

2. Establishment of integrated prediction model

2.1. Trajectory similarity based prediction

The TSBP algorithm can compare the characteristic quantity parameters with the historical data. The most similar one or several trajectories can be selected as reference values to predict the RUL of mills. In the milling process, there are many parameters, including cutting force, cutting parameters and so on, closely related with the RUL of mill. Since the multi-dimensional data is too large, it will greatly increase the computational complexity, which is a challenge to the computer. Therefore, it is necessary to convert the multi-dimensional parameter into one-dimensional parameter. In this paper, the experimental data will

be normalized, and the different feature quantities will be converted into the same attribute. The minimum-maximum specification method is adopted, and the calculation method is:

$$\tilde{d}_{iQ} = \frac{d_{iQ} - \min(Q)}{\max(Q) - min(Q)} * 2 - 1 \quad (1)$$

where d_{iQ} is the size of the characteristic quantity i on the attribute Q.

The basic idea of the TSBP algorithm is: if the degradation index of the sample $Z = (z_1, z_2, \ldots, z_r)$ to be predicted is similar to the performance degradation trend of the reference sample T during a certain period of time (T_p, T_{p+r}), the remaining life of the sample should also be the same as the *RUL* of the reference sample. The process of this model is as follows:

(1) Fit the normalized data, and build all the fitted curves into a pattern library G:

$$G : z = g(t) \quad (2)$$

(2) Use the normalized Euclidean distance function as a similarity measure function, define the distance function as follows:

$$d(Z, G_i, p) = \sum_{j=1}^{r} \frac{(z_j - g_i(p + t_j))^2}{\sigma_i^2} \quad (3)$$

where the similarity between the device Z to be predicted and the reference mode G_i in $[p, p + r]$ is represented as $d(Z, G_i, p)$, and p represents the first sampling point in the reference mode in which the similarity calculation is performed, and the range of p is $0 \le p \le T_i - r + 1$. σ^2 shows the prediction variance of the reference pattern G_i.

(3) Find the smallest p in the sample library and find the *RUL* of the tool:

$$RUL_i = \arg\min_p d(Z, G_i, p) \quad (4)$$

(4) At the same time, we can know that the shortest distance from the current mode is:

$$D_i = \min d(Z, G_i, p) \quad (5)$$

(5) The similarity-based approach suggests that a high-similarity reference model can provide useful information. If two devices have the same degradation trend, the remaining life will be closer. This paper uses the following weight calculation method:

$$w_i = 1 - \frac{D_i}{\sum_{i=1}^{N} D_i} \quad (6)$$

(6) The formula for calculating the remaining life of the tool can be expressed as:

$$RUL = \sum_{i=1}^{N} w_i \cdot RUL_i \quad (7)$$

where N is the number of reference patterns in the pattern library, and w_i is the weight of the i^{th} pattern.

2.2. Integrated predictive model

SVR is a generalized model of support vector machine. The basic idea is to find an optimal plane in a specific feature space so that the distance between all training samples and the classification surface is minimum. This paper uses Adaboost-based learning device to integrate TSBP and SVR algorithms. The Adaboost promotion method is a commonly used integrated learning algorithm. The core idea is to use the same training set data to train different weak learners. Then the Adaboost promotion method integrates these weak learners, continuously updates the sample weights and learner weights, and constructs a stronger learner. It will increase the weight of the sample which is predicted to be wrong in the last round of training, and reduce the weight of the sample which is predicted in the previous round of training. If the correct sample is not predicted, the next round will go on due to the larger weight. More attention is paid to the reinforcement of the samples that are easily predicted inaccuracy, and the performance of the weak learner is improved. Finally, a series of weak learners are weighted and linearly combined to obtain a strong learner. The base learners are promoted to strong learners on the verification set, and finally the performance of the model is further tested on the test set. The integrated predictive model flow is shown in Fig. 1.

In order to evaluate the accuracy of the integrated model prediction results, the following four evaluation indicators are selected in this paper:

Mean Absolute Error (MAE)

$$MAE = \frac{1}{N} \sum_{i=1}^{N} |r_i^* - r_i| \quad (8)$$

Root Mean Squared Error (*RMSE*)

$$RMSE = \sqrt{\frac{1}{N} \sum_{i=1}^{N} (r_i^* - r_i)^2} \quad (9)$$

Normalized Mean Squared Error (*NMSE*)

$$NMSE = \frac{N - 1}{N \sum_{i=1}^{N} \left(r_i - \bar{r}\right)^2} \sum_{i=1}^{N} (r_i^* - r_i)^2 \quad (10)$$

SCORE

$$S_n = \begin{cases} e^{r_n - r_n^*/13} - 1, r_n^* \le r_n \\ e^{r_n^* - r_n/10} - 1, r_n^* > r_n \end{cases}, \; SCORE = \sum_{n=1}^{N} S_n \quad (11)$$

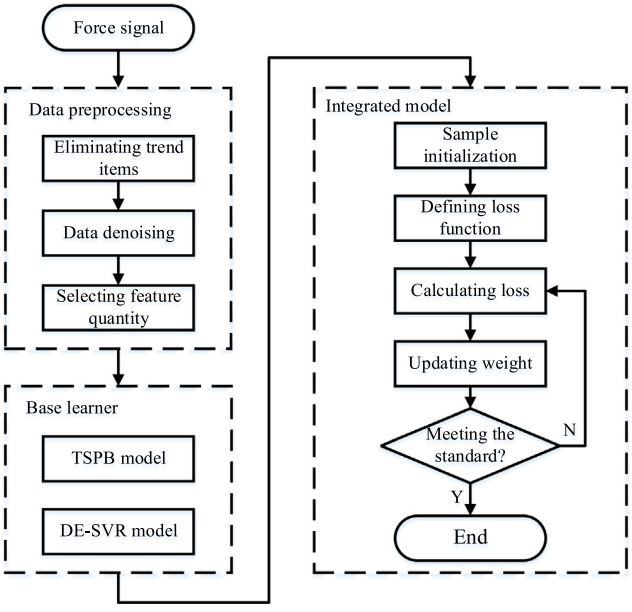

Fig. 1. Integrated predictive model predicting process.

where r^* is predictive value, r is real value, is average value. The lower the value, the higher the prediction accuracy of the model, N is number of value.

3. Experiment set-up and procedure

3.1. Experiment set-up

The CNC milling tool produced by Zhongjie company has the maximum spindle speed of 6000 rpm. The workpiece material used for the experiment is TC4 and the size is 60 mm × 60 mm × 40 mm. The main chemical compositions and contents of TC4 are shown in Table 1 and the main material properties of TC4 are shown in Table 2. The dynamometer is Kistler 9625B and the sensitivity of the x/y axis is 9 pC/N. A small vise is used to clamp the workpiece. The vise is fixed on the dynamometer, and the dynamometer is bolted to the workbench. The actual photograph and illustration of experiment set-up is shown in Fig. 2. This paper selects three sample tools during the milling experiment for analysis. The specific information of each sample tool is shown in Table 3.

3.2. Design of experiment

The cutting method is down-milling without cutting fluid, and straight along the y-axis of the machine tool. The each cutting distance is 60 mm. The cutting parameters of each sample tool are shown in Table 4. The sampling frequency of the dynamometer is 1000 Hz for the whole process.

3.3. Tool wear measurement

During the process of machining TC4, there are many wear forms, including the flank wear and the rake wear, and the boundary wear is also serious. The flank wear directly affects the machining accuracy of the workpieces, and is easy to measure, so the average width of the flank wear of the tool is measured by the

Table 1
The main chemical compositions and contents of TC4.

Chemical compositions	Fe	C	N	H	O	Al	V	Ti
Contents (%)	0.40	≤0.10	≤0.10	≤0.015	≤0.3	5.5 ~ 6.7	3.5 ~ 4.5	margin

Table 2
The main material properties of TC4.

Material properties	Hardness	Density (kg/m^3)	Melting Point (°C)	Elastic Modulus (GPa)	Poisson Ratio μ
Values	HRC30	4430	1605	113	0.34

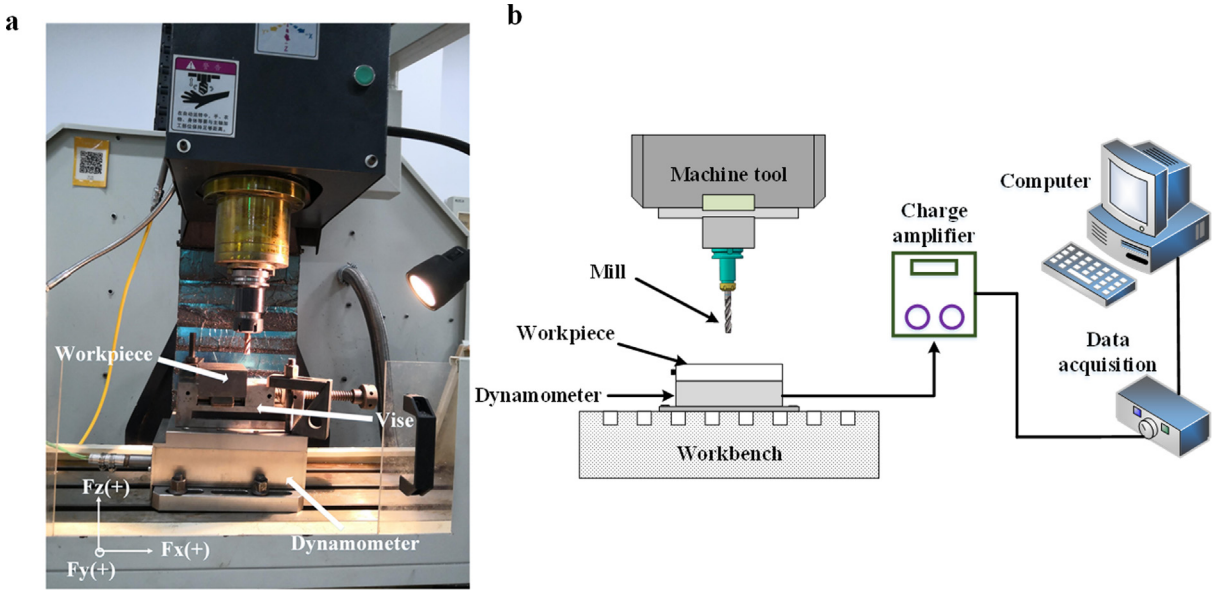

Fig. 2. Experimental set-up for milling, a. actual set-up, b. illustration.

Table 3
Sample tool information.

Number	Type	Coat	Tool radius (mm)	Rake (°)	Clearance (°)	Diameter (mm)	Specification (mm)	Teeth
1	Solid carbide	–	0.4	5°~9°	11°	8	8 × 8 × 19 × 63	4
2	Solid carbide	–	0.4	5°~9°	11°	10	10 × 10 × 22 × 72	
3	Coated cemented carbide	TiN	0.4	5°~9°	11°	10	10 × 10 × 22 × 72	

Table 4
Cutting parameters of each sample tool.

No.	Cutting speed (m/min)	Feed per tooth (mm/z)	Radial depth (mm)	Axial depth (mm)
1	25	0.015	3	5
2	31	0.02	3	5
3	31	0.02	2	5

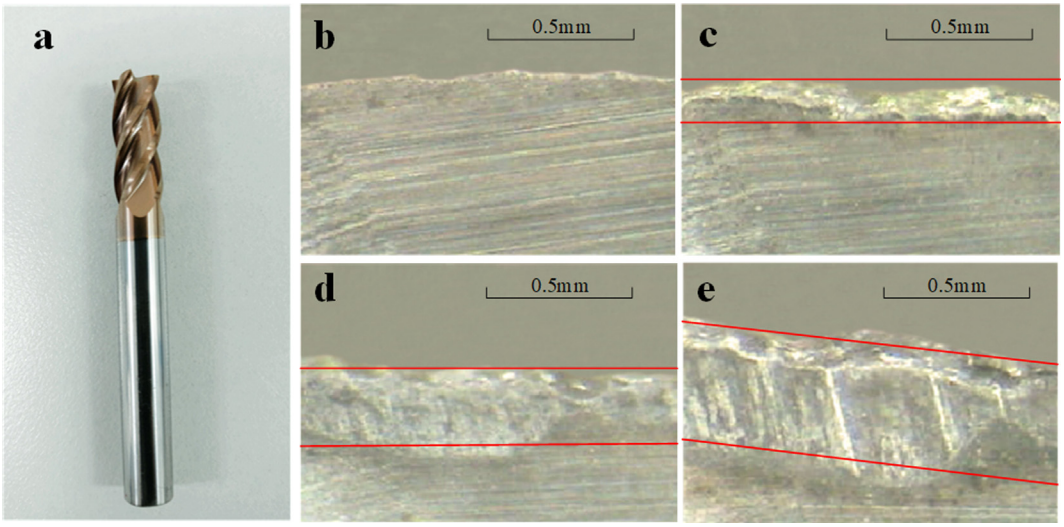

Fig. 3. The overall appearance and wear morphology of Tool 3, a. The overall appearance of Tool 3, b. VB = 0 mm, c. VB = 0.14 mm, d. VB = 0.26 mm, e. VB = 0.40 mm.

VHX-500 microscope to evaluate tool wear. In the ISO 3685 standard, the tool is determined as failure when the current tool flank wear value reaches 0.4 mm. The cutting parameters of each tool remain unchanged from the initial state to the failure state in the milling process. When the cutting distance is 120 mm, the value of the tool wear is recorded by taking photos with the microscope. The overall appearance and wear morphology of Tool 3 are shown in Fig. 3. Tool wear is slight in the initial stage of machining TC4 and tool wear increases along with processing. Groove wear appears in the late stage. It's a typical progressive wear.

4. Results and discussion

4.1. Analysis of the cutting force signal

4.1.1. Time domain analysis

As the amount of wear increases, the tool-workpiece contact surface becomes more and more unstable, which increases the friction between the two contacting surfaces and the cutting force. The cutting performance of the tool will drop sharply after a threshold, which will cause problems such as the surface quality of the parts being reduced or even broken. The average values of the flank wear on the 4 teeth are calculated as VB values of Tool 1, Tool 2, Tool 3. The relationship between VB value and cutting distance is shown in Fig. 4.

The change of VB value of the cutting tool has three stages: initial stage, steady stage and sharp stage. The corresponding the cutting distance of each stage is shown in Table 5. In the initial stage, the tool wear increases fast because the new cutting edge is sharp, the tool-workpiece contact area is small. The tool-workpiece contacting area becomes larger in steady stage, so the cutting force enters a steady stage. Once exceeding the threshold, the cutting force will increase sharply because the tool wear increases rapidly and becomes dull.

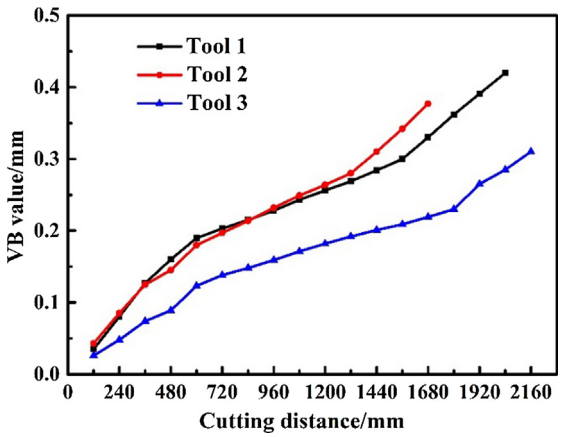

Fig. 4. The relationship between VB value and cutting distance.

The relationship between the root mean square value (*RMSV*), average value (*AV*), standard deviation value (*SDV*) of the cutting force and VB value is shown in Fig. 5. When the tool wear increases, the characteristic quantity of the cutting force is gradually increased, which can also be divided into three stages: initial stage, steady stage and sharp stage. The characteristic quantity increases rapidly when VB value is in the range of $0 \sim 0.16$ mm, $0 \sim 0.18$ mm and $0 \sim 0.12$ mm for Tool 1, Tool 2 and Tool 3, respectively. The characteristic quantity increases steadily when VB value is in the range of $0.16 \sim 0.3$ mm, $0.18 \sim 0.28$ mm and $0.12 \sim 0.25$ mm for Tool 1, Tool 2 and Tool 3, respectively. The characteristic quantity increases sharply when VB value is in the range of $0.3 \sim 0.42$ mm, $0.28 \sim 0.37$ mm and $0.25 \sim 0.31$ mm for Tool 1, Tool 2 and Tool 3, respectively. The results show that there is a certain relationship between three characteristic quantities (*RMSV/AV/SDV*) of the cutting force and VB value. They can be used to monitor the tool wear.

Table 5
The corresponding the cutting distance of each stage.

No.	Name	Initial stage	Steady stage	Sharp stage
1	Cutting distance/mm	0 ~ 480	480 ~ 1560	1560 ~ 2040
	VB/mm	0 ~ 0.16	0.16 ~ 0.3	0.3 ~ 0.42
2	Cutting distance/mm	0 ~ 600	600 ~ 1320	1320 ~ 1680
	VB/mm	0 ~ 0.18	0.18 ~ 0.29	0.29 ~ 0.38
3	Cutting distance/mm	0 ~ 600	600 ~ 1800	1800 ~ 2160
	VB/mm	0 ~ 0.13	0.13 ~ 0.23	0.2 ~ 0.33

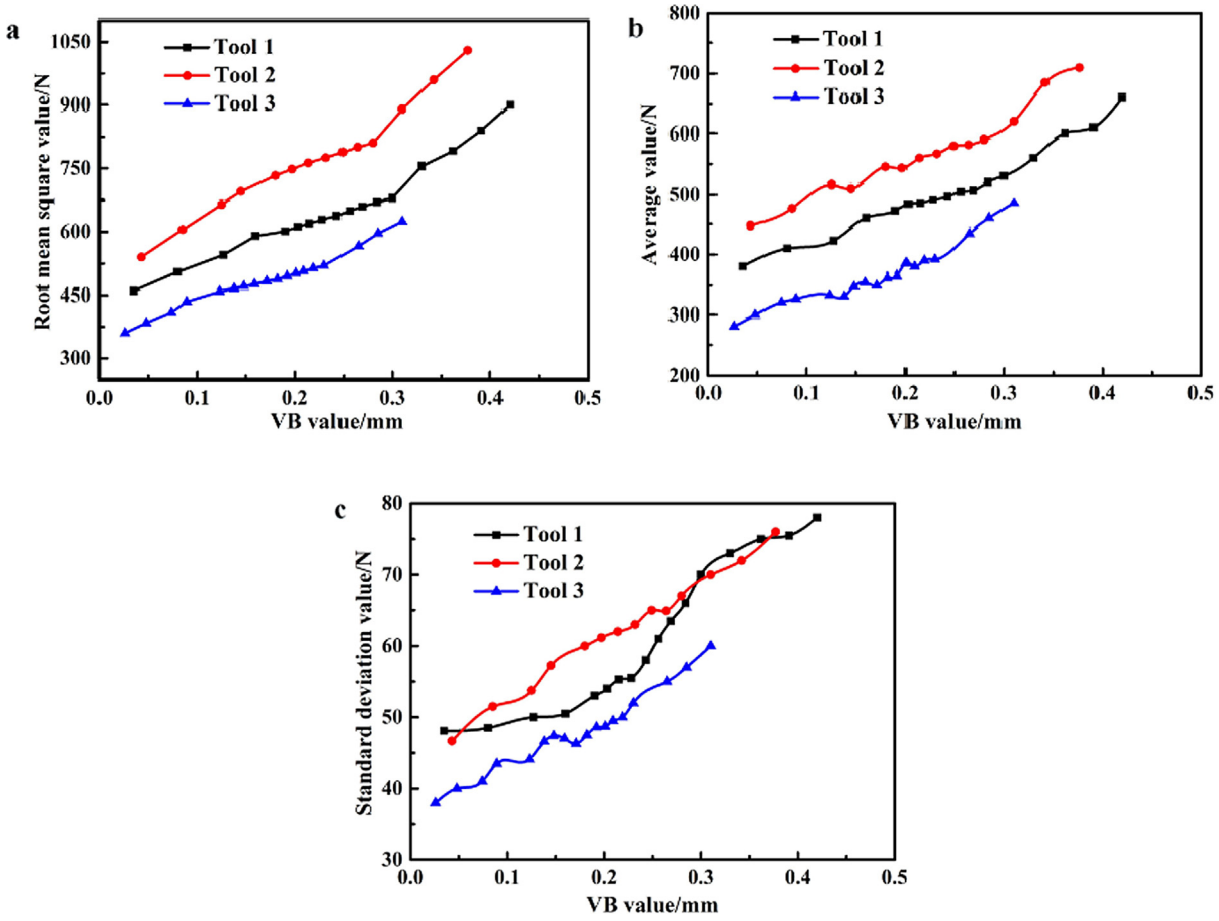

Fig. 5. The relationship between each characteristic quantity of the cutting force and VB value, a. the relationship between *RMSV* and VB value, b. the relationship between *AV* and VB value, c. the relationship between *SDV* and VB value.

4.1.2. Wavelet analysis

According to principle, if the signal is subjected to *n*-layer wavelet decomposition, 2*n* frequency bands can be obtained. Let f_s be the signal sampling frequency. The frequency range of each frequency band is as follows:

$$\left[0,\frac{f_s}{2^{n+1}}\right],\left[\frac{f_s}{2^{n+1}},\frac{2f_s}{2^{n+1}}\right],\left[\frac{2f_s}{2^{n+1}},\frac{3f_s}{2^{n+1}}\right],\left[\frac{3f_s}{2^{n+1}},\frac{4f_s}{2^{n+1}}\right],\cdots,\left[\frac{(2^n-1)f_s}{2^{n+1}},\frac{f_s}{2}\right] \tag{12}$$

3-layer wavelet packet decomposition is used in this paper. The signals of x and y direction of Tool 3 is decomposed into eight frequency bands by using the db3 wavelet packet. The frequency ranges are (Hz): [0, 62.5], [62.5, 125], [125, 187.5], [187.5, 250], [250, 312.5], [312.5, 375], [375, 437.5], [437.5, 500]. The ratio of the energy distribution of each frequency band to the total energy is shown in Fig. 6. It can be found that whether the initial or late stage of Tool 3, the signal energy of low frequency band is main.

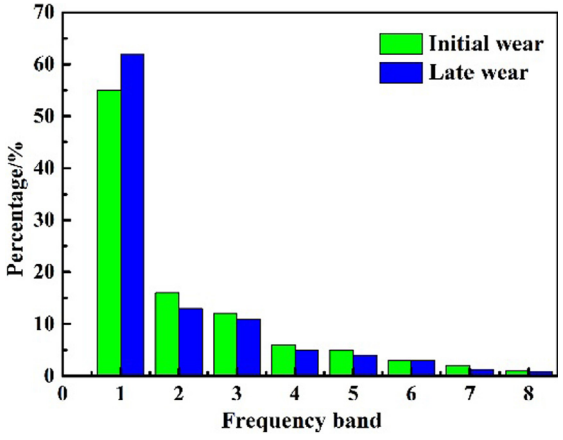

Fig. 6. The ratio of the energy distribution of each frequency band to the total energy.

In order to further explore the relationship between the characteristic quantity of signal energy and Tool 3 wear, the three-dimensional energy which is obtained by wavelet packet decomposition is calculated under different amounts of wear, as shown in Figs. 7–9. As the tool wear increases, the energy values increase, and the change between the sharp wear stage and the tool breakage stage is obvious. A critical point is existed in the cutting process. When the tool wear exceeds this critical point, the energy value of the force signal increases much faster than the normal period. It can be preliminarily judged that the energy

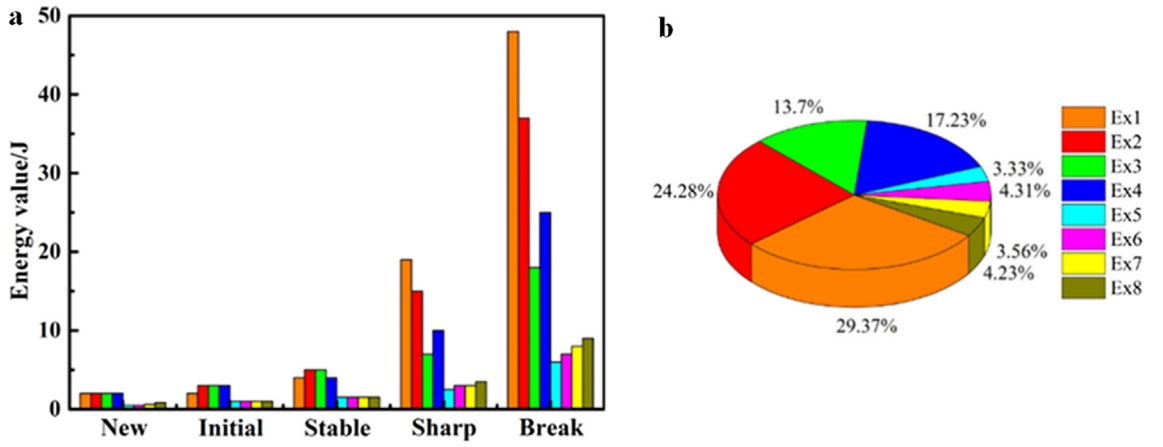

Fig. 7. Distribution and proportion of energy of *x*-directional force for Tool 3, a. the distribution of energy in each frequency band in different tool wear stages, b. the proportion of energy in each frequency band.

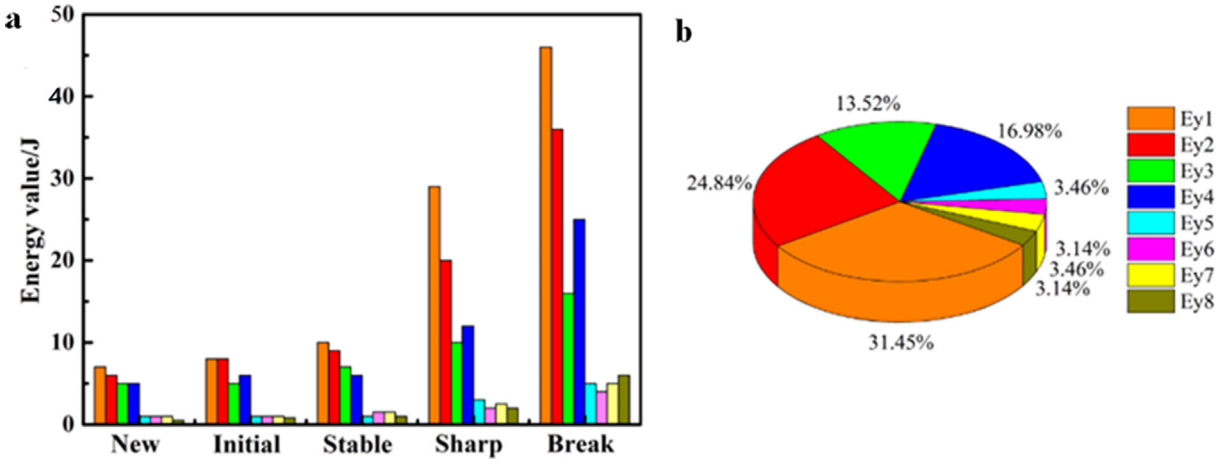

Fig. 8. Distribution and proportion of energy of *y*-directional force for Tool 3, a. the distribution of energy in each frequency band in different tool wear stages, b. the proportion of energy in each frequency band.

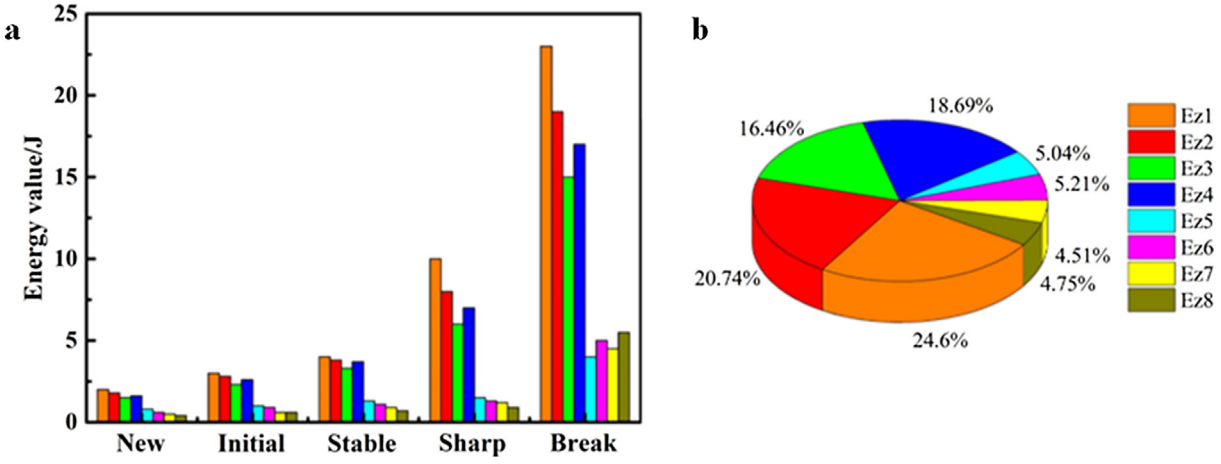

Fig. 9. Distribution and proportion of energy in *z*-directional force for Tool 3, a. the distribution of energy in each frequency band in different tool wear stages, b. the proportion of energy in each frequency band.

value is strongly related with current tool state, and can be used as a characteristic quantity to monitoring the tool wear. At the same time, it also reflects that the three-layer wavelet packet decomposition selected in this paper is suitable, and the detailed information of the force signal is included with fewer decomposition layers. According to Figs. 7–9, the energy of the 1 ~ 4 frequency bands accounts for more than 3/4 energy of all frequency bands, therefore, the cutting force signal is selected from the 1 ~ 4 frequency bands in this section. The *SDV* of the energy values in different tool wear stages is shown in Fig. 10. The abscissa is divided into five stages according to the amount of wear of Tool 3: new tool, initial, stable, sharp and breakage. The corresponding VB values in each stage are: 0 ~ 0.074 mm, 0.074 ~ 0.138 mm, 0.138 ~ 0.209 mm, 0.209 ~ 0.265 mm, 0.265 ~ 0.310 mm.

It can be seen from Fig. 10 that the *SDV* of the energy values of the four frequency bands increases when the tool wear increases, and increase rate in the later stage of wear is significantly larger than the rate in the early wear stage. There is a sudden change of the *SDV* in the sharp wear point. The *SDV* of the energy value is strongly correlated with VB value and can reflect the state of the tool during the cutting process.

4.2. Selection of characteristic quantity

In this paper, time domain and wavelet analysis are carried out by using data of Tool 3. In time domain analysis stage, the relationship between *AV*, *RMSV* and *SDV* of the cutting force and VB value are analyzed. In the wavelet analysis stage, the energy values of 8 frequency bands and the *SDV* of energy values of 4 frequency bands are analyzed. Since the signal has three directions: *x*, *y*, and *z*, there are 9 characteristic quantities in the time domain field and 36 characteristic quantities in wavelet analysis field.

In order to further explore the degree of correlation between these signal characteristic quantities and VB value, this paper analyzes the correlation between the two factors, and judges the fitting degree of the characteristic quantity in different states of tool by the magnitude of the correlation coefficient. The calculation formula is as follow:

$$R_{xy} = \frac{Cov(x,y)}{\sqrt{Var(x)Var(y)}} \tag{13}$$

where x represents a certain characteristic quantity of the signal and y represents VB value of the tool. R_{xy} represents the correlation coefficient which is between −1 and 1. When $R_{xy} \in [-1, 0)$, it indicates a negative correlation; when $R_{xy} \in (0, 1]$, it indicates a positive correlation. The larger the R_{xy} is, the stronger the correlation is; when $R_{xy} = 0$, it indicates that there is no correlation.

By analyzing the characteristic quantities, the tool wear and RUL could be predicted by the integrated prediction model proposed in this paper. Guaranteeing a strong correlation between characteristic quantity and the tool wear is a prerequisite for ensuring prediction accuracy, and the correlation coefficient corresponding to each characteristic quantity of Tool 3 is shown in Table 6. *x*, *y*, and *z* represent three directions. The number of the characteristic quantity is the frequency band in the wavelet analysis stage, for example, *E3-y* is the energy in the frequency band 3 of *y* direction.

The following characteristic vectors are used in the prediction model according to Table 4:

$$\alpha_1 = [RMSV - x, RMSV - y, RMSV - z] \tag{14}$$

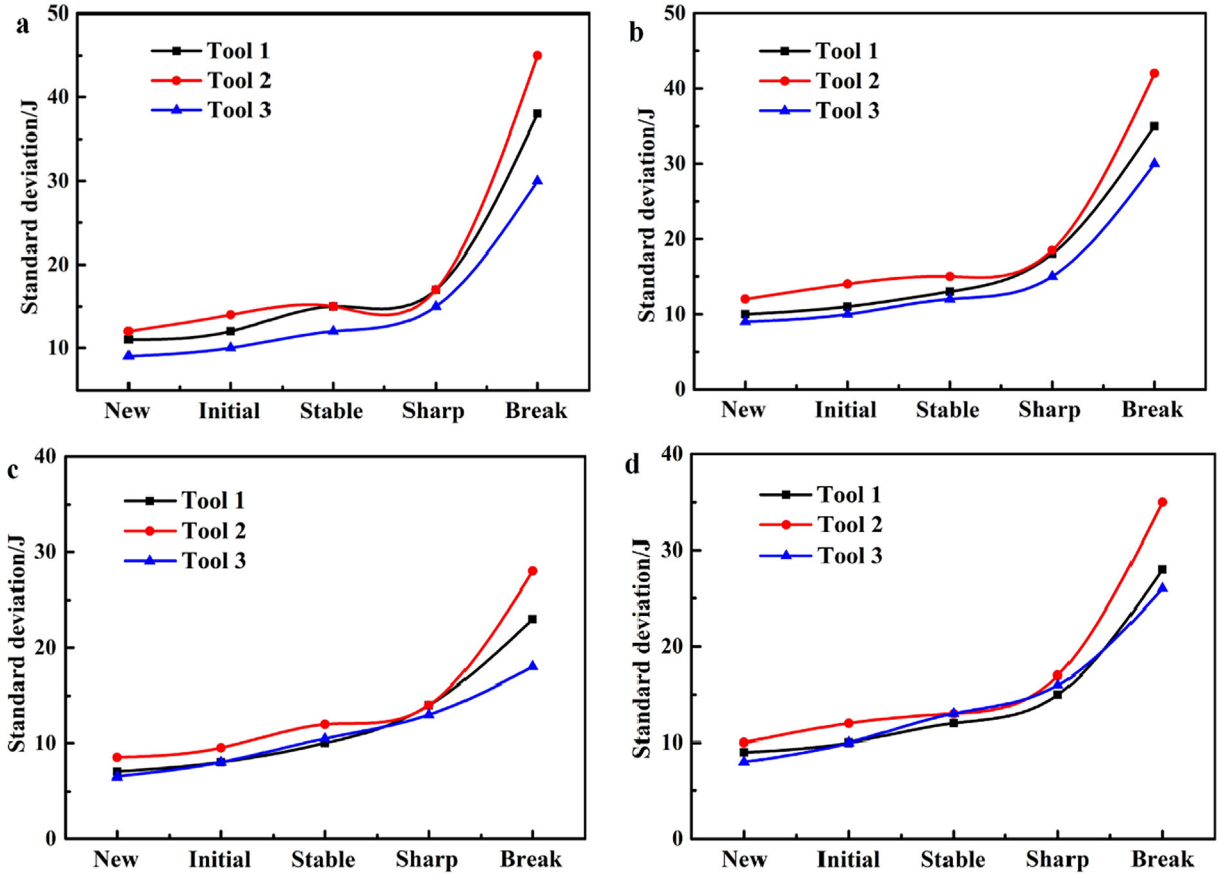

Fig. 10. Standard deviation of energy values for different wear periods in the 1 ~ 4 frequency bands, a. the frequency band 1, b. the frequency band 2, c. the frequency band 3, d. the frequency band 4.

Table 6
R_{xy} between characteristic quantity and VB value.

Characteristic quantity	R_{xy}	Characteristic quantity	R_{xy}	Characteristic quantity	R_{xy}	Characteristic quantity	R_{xy}
AV-x	**0.796**	*E2-x*	0.812	*E6-x*	0.705	σ2-*x*	0.772
AV-y	**0.812**	***E2-y***	**0.853**	***E6-y***	**0.743**	**σ2-*y***	**0.819**
AV-z	**0.783**	*E2-z*	0.697	*E6-z*	0.632	σ2-*z*	0.725
RMSV-x	**0.852**	***E3-x***	**0.857**	***E7-x***	**0.718**	σ3-*x*	0.764
RMSV-y	**0.861**	*E3-y*	0.807	*E7-y*	0.705	**σ3-*y***	**0.817**
RMSV-z	**0.801**	*E3-z*	0.685	*E7-z*	0.585	σ3-*z*	0.696
SDV-x	**0.835**	***E4-x***	**0.834**	*E8-x*	0.673	**σ4-*x***	**0.794**
SDV-y	**0.864**	*E4-y*	0.795	***E8-y***	**0.696**	σ4-*y*	0.758
SDV-z	**0.767**	*E4-z*	0.674	*E8-z*	0.597	σ4-*z*	0.680
E1-x	0.881	***E5-x***	**0.802**	σ1-*x*	0.783		
E1-y	**0.932**	*E5-y*	0.741	**σ1-*y***	**0.827**		
E1-z	0.728	*E5-z*	0.627	σ1-*z*	0.731		

The bold portion is a large correlation coefficient, which will be used as a characteristic quantity for evaluating the accuracy of the cutting tool wear and life prediction algorithm.

$$\alpha_2 = [AV - x, AV - y, AV - z] \tag{15}$$

$$\alpha_3 = [SDV - x, SDV - y, SDV - z] \tag{16}$$

$$\alpha_4 = [\sigma 1 - y, \sigma 2 - y, \sigma 3 - y, \sigma 4 - x] \tag{17}$$

$$\alpha_5 = [E1 - y, E2 - y, E3 - x, E4 - x, E5 - x, E6 - y, E7 - x, E8 - y] \tag{18}$$

4.3. Training and performance evaluation of prediction model

4.3.1. Model training

Due to the limitation of experimental condition, the training of the integrated predictive model is carried out through the public data set PHM Society (2010). The equipment is Roders Tech RFM760 high-speed CNC cutting center. The tungsten carbide ball-end mill is used to cut stainless steel material. The hardness of the work-piece is HRC52. The cutting parameters of each tool from in the entire milling process are kept same. The specific parameters during the cutting process are shown in Table 7.

The training error is set to 10^{-3}, and the number of training sample is 2700. The training results are shown in Fig. 11.

4.3.2. Performance evaluation

The signal characteristic vectors α1, α2, α3, α4, α5 of sample tool are used to predict VB value and RUL of tool in this section. The relative error and evaluation index are carried out. The integrated predictive model can continue to learn the collected signals to improve the prediction accuracy of established model. The strong learner that can continuously adjust the weight of each signal characteristic quantity according to the change of characteristics is used in this model.

VB value prediction results of the sample tool are shown in Fig. 12. The overall prediction stage is effective, and the trend of predicted value curve is roughly similar to the measured value curve. The relative errors of VB value prediction results of the sample tool at different process stages are shown in Fig. 13. The prediction accuracy in the stable stage of wear is above 88%, reflecting the good accuracy and adaptability of the prediction model. The relative error in the early stage of wear is large because the cutting time is short which causes that the amount of data collected is limited, so the prediction accuracy is not high. The relative error of prediction accuracy in the later stage of wear decreases because the deterioration of the tool flank wear, which causes the sharp force increase and the faster tool wear rate.

The evaluation index values of the integrated prediction model are shown in Table 8. At the same time, the TSPB and DE-SVR single model, as well as the PSO-SVM model and HMM model are compared.

The integrated prediction model proposed in this paper is not the same as the TSPB model in the *NMSE* index, and the other three indexes are the best. The *NSME* reflects the degree of oscillation of the data, and is sensitive to abnormal data. The large amount of signal change after the tool wear could bring about a large prediction bias. However, considering the four indexes, the integrated model proposed in this paper is best.

The RUL prediction results of the sample tool are shown in Fig. 14. The predicted value fluctuates around the actual value, and the overall change remains the same. When the integrated predictive model has been trained, it has good adaptability and

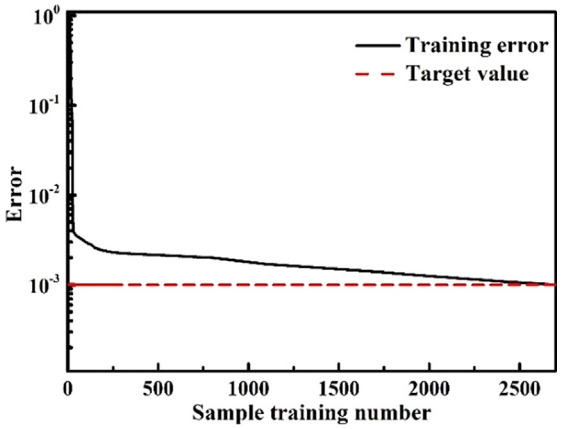

Fig. 11. The convergence curve for training sample error.

Table 7
The cutting parameters for public data set.

No.	Spindle speed (rpm)	Feed per tooth (mm/z)	Radial depth(mm)	Axial depth(mm)
1	8000	0.02	2	5
2	10,000	0.025	3	5
3	12,000	0.03	3	5

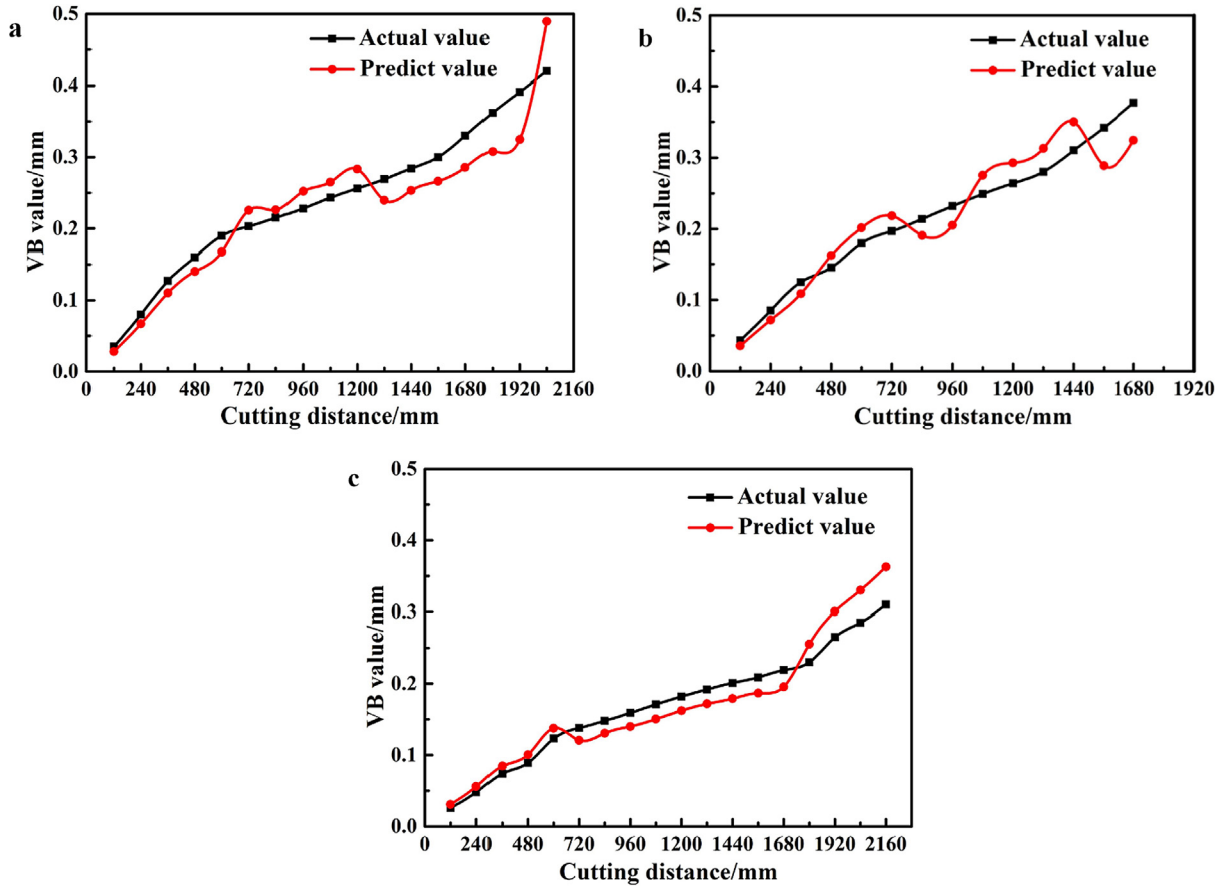

Fig. 12. Predicted and actual VB values of sample tool, a. predicted and actual VB values of Tool 1, b. predicted and actual VB values of Tool 2, c. predicted and actual VB values of Tool 3.

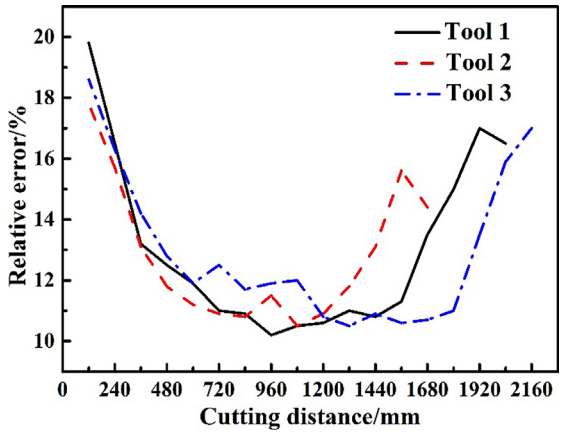

Fig. 13. The relative error of VB value prediction results.

Table 8
Evaluation index of VB value prediction results.

Name	*MAE*	*NMSE*	*RMSE*	*SCORE*
TSPB	16.73	**19.89**	0.29	653.9
SVR	18.89	22.64	0.19	816.2
PSO-SVM	17.03	21.97	0.52	984.3
HMM	19.51	25.32	0.27	679.8
TSPB-SVR	**14.65**	20.35	**0.18**	**570.1**

The bold numbers are optimal values of each evaluation index.

accuracy of life prediction for different tools or cutting parameters. According to Fig. 14a, the model has a good predictive effect on Tool 1. From the beginning to the end of the cutting process, the predicted value always fluctuates above or below the actual value, and the tool life prediction value is closer to the actual value in the later cutting process. According to Fig. 14b, in the 0 ~ 720 mm cutting distance interval, the life prediction value of Tool 2 is smaller than the actual value, and the error of prediction result is relatively large. As the cutting progresses, the amount of the cutting force data collected increases continuously, and the prediction accuracy is continuously improved through continuous learning. When the cutting distance is larger than 720 mm, life prediction value has been fluctuating around the actual value because the prediction accuracy is continuously improving. According to Fig. 14c, the life prediction value of Tool 3 is always smaller than the actual value during the cutting distance phase of 0 ~ 360 mm. In the cutting distance stage of 360 ~ 960 mm, the predicted value is always larger than the actual value, and the predicted value after 960 mm has been fluctuating around the actual value, maintaining a high prediction accuracy.

The relative error of prediction results of the RUL at different cutting distance stages is shown in Fig. 15. In the initial stage, due to the small amount of collected data, the change of characteristic quantity of the signal is not accurate, and the relative error of prediction result of the integrated model is large. The relative error of Tool 1, Tool 2, Tool 3 is from 12% to 21%, 13% to 22%, 10% to 19.5% respectively. In the stable stage, the amount of data collected is significantly increased. The integrated prediction model has improved the prediction accuracy from the previous stage through the previous prediction and learning. The relative error of Tool 1,

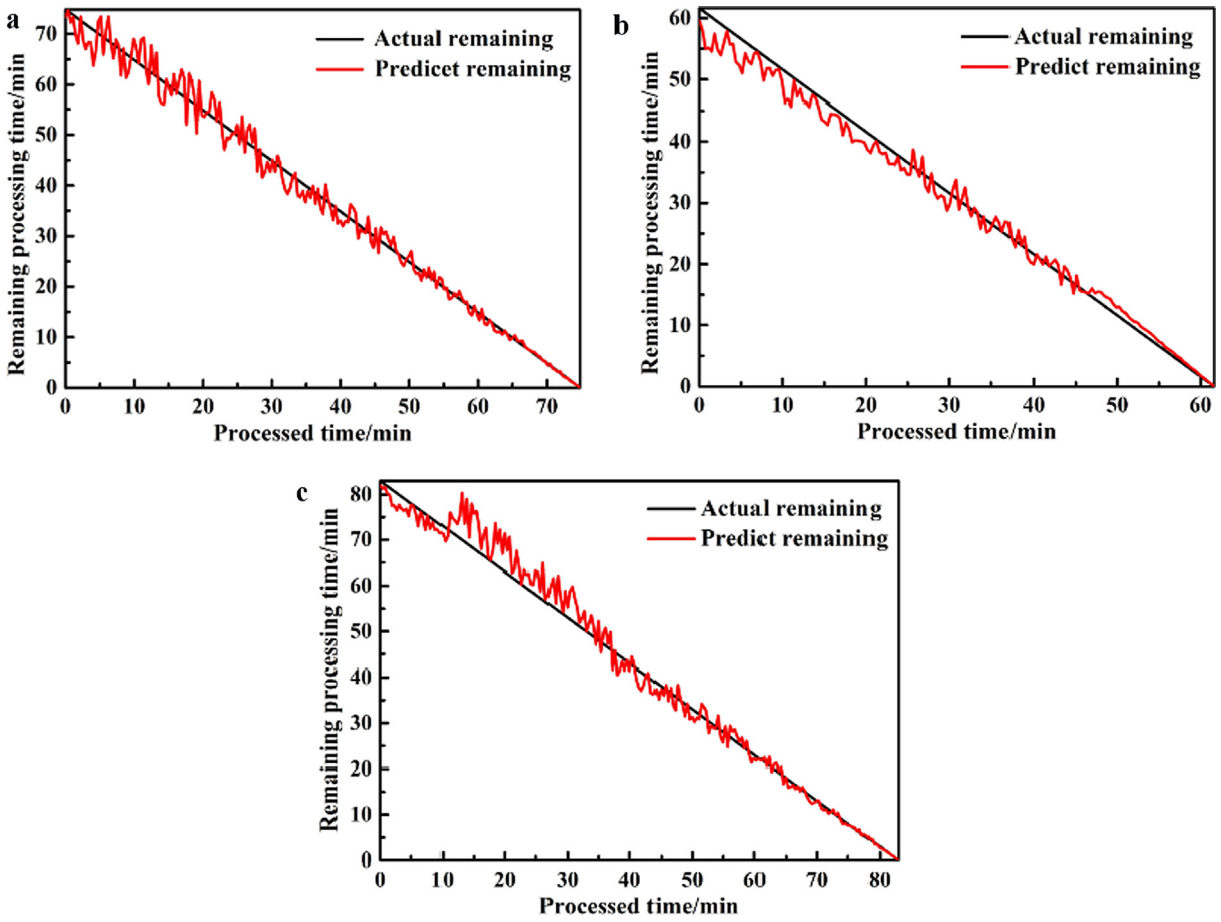

Fig. 14. Predicted and actual life values of sample tool, a. predicted and actual life values of Tool 1, b. predicted and actual life values of Tool 2, c. predicted and actual life values of Tool 3.

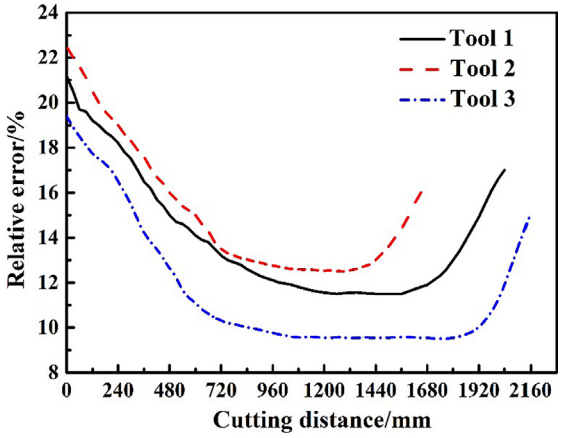

Fig. 15. The relative error of the RUL prediction results.

Tool 2, Tool 3 is stable at around 88.5%, 87.5%, 90.5% in this stage respectively. As the cutting distance increases, the integrated model predicts the RUL of tool more accurately because the prediction model can more accurately fit the change of the signal characteristic quantity as the cutting distance increases and the amount of collected data increases. In the last stage, although the amount of data has increased greatly, the relative error has been increased. This is due to the sharp wear of the tool in this stage which causes a large change of cutting force signal, resulting in a decrease in the prediction accuracy of the integrated model.

Table 9
Evaluation index of model the RUL prediction results.

Name	*MAE*	*NMSE*	*RMSE*	*SCORE*
TSPB	21.89	34.29	0.47	746.8
SVR	25.61	30.46	0.30	695.3
PSO-SVM	**19.43**	35.48	0.21	807.6
HMM	23.89	36.52	0.29	733.4
TSPB- SVR	20.92	**27.46**	**0.25**	**615.2**

The bold numbers are optimal values of each evaluation index.

The evaluation index values of the integrated prediction model are shown in Table 9. At the same time, the TSPB and DE-SVR single model, as well as the PSO-SVM model and HMM model are compared. It can be seen that the indexes of *NMSE*, *RMSE*, and *SCORE* for the integrated model have the lowest value which indicates the best prediction accuracy when compared with other four models. The *MAE* index of the integrated model is slightly inferior to the PSO-SVM. In summary, the prediction performance of the RUL of the integrated prediction model established in this paper is better than other four models.

5. Conclusion

In order to predict tool wear and the remaining life, this paper proposes an integrated prediction model based on trajectory similarity and support vector regression fusion prediction model. By analyzing cutting force signals obtaining in milling TC4 workpieces, following results are found:

- There is a certain relationship between three characteristic quantities (*RMSV/AV/SDV*) of cutting force signals and VB values and they can be used to monitor the tool wear. The *SDV* of the energy values of the four frequency bands increases when the tool wear increases, and increase rate in the later stage of wear is significantly larger than the rate in the early wear stage. There is a sudden change of the *SDV* in the sharp wear point. The *SDV* of the energy value is strongly correlated with VB value and can reflect the state of the tool during the cutting process.
- Four evaluation indicators (MAE/RMSE/NMSE/SCORE) are selected to compare the prediction accuracy of the integrated model with the prediction accuracy of the single algorithm. In summary, the prediction performance of the tool wear and RUL of the integrated prediction model established in this paper is better than other four models.
- The relative errors of VB value prediction accuracy in the stable stage of the sample tool is above 88%, reflecting the good accuracy and adaptability of the prediction model. The RUL prediction accuracy of the stable stage of Tool 1, 2, and 3 is 88.5%, 87.5%, and 90.5% respectively by using this integrated prediction model. These results show that the integrated prediction model can be used to monitor tool wear practically to a certain extent and the performance of model can be improved by continue learning the collected signals.

Acknowledgements

The authors would like to thank the National Natural Science Foundation of China (U1601204) and National Natural Science Foundation of Jiangsu Province (BK20180435) for financial supports.

References

[1] C.H. Lim, M.J. Kim, J.Y. Heo, K.J. Kim, Design of informatics-based services in manufacturing industries: case studies using large vehicle-related databases, J. Intell. Manuf. 29 (2018) 497–508.
[2] G. Malayath, S. Katta, A.M. Sidpara, S. Deb, Length-wise tool wear compensation for micro electric discharge drilling of blind holes, Measurement 134 (2019) 888–896.
[3] X. Liang, Z. Liu, B. Wang, State-of-the-art of surface integrity induced by tool wear effects in machining process of titanium and nickel alloys: a review, Measurement 132 (2019) 150–181.
[4] C. Wang, Z. Bao, P. Zhang, W. Ming, M. Chen, Tool wear evaluation under minimum quantity lubrication by clustering energy of acoustic emission burst signals, Measurement 138 (2019) 256–265.
[5] A.H. Musfirah, J.A. Ghani, C.H.C. Haron, Tool wear and surface integrity of inconel 718 in dry and cryogenic coolant at high cutting speed, Wear 376–377 (2017) 125–133.
[6] H. Zeng, R. Yan, P. Du, M. Zhang, F. Peng, Notch wear prediction model in high speed milling of AerMet100 steel with bull-nose tool considering the influence of stress concentration, Wear 408–409 (2018) 228–237.
[7] A. Kumar, S. Kaminski, S.N. Melkote, C. Arcona, Effect of wear of diamond wire on surface morphology, roughness and subsurface damage of silicon wafers, Wear 364–365 (2016) 163–168.
[8] M. Aramesh, Y. Shaban, S. Yacout, H.H.A. Attia, M. Kishawy, Balazinski, Survival life analysis applied to tool life estimation with variable cutting conditions when machining titanium metal matrix composites, Mach. Sci. Technol. 20 (2016) 132–147.
[9] N.R. Dhar, M. Kamruzzaman, M. Ahmed, Effect of minimum quantity lubrication (MQL) on tool wear and surface roughness in turning AISI-4340 steel, J. Mater. Process. Technol. 172 (2006) 299–304.
[10] R.W. Maruda, G.M. Krolczyk, S. Wojciechowski, K. Zak, W. Habrat, P. Nieslony, Effects of extreme pressure and anti-wear additives on surface topography and tool wear during MQCL turning of AISI 1045 steel, J. Mech. Sci. Technol. 32 (2018) 1585–1591.
[11] P. Twardowski, S. Wojciechowski, M. Wieczorowski, T. Mathia, Surface roughness analysis of hardened steel after high-speed milling, Scaning 33 (2011) 386–395.
[12] M.M. De Aguiar, A.E. Diniz, R. Pederiva, Correlating surface roughness, tool wear and tool vibration in the milling process of hardened steel using long slender tools, Int. J. Mach. Tools Manuf. 68 (2013) 1–10.
[13] S. Wojciechowski, K. Mrozek, Mechanical and technological aspects of micro ball end milling with various tool inclinations, Mech. Sci. 134 (2017) 424–435.
[14] G. Zhang, S. To, G. Xiao, The relation between chip morphology and tool wear in ultra-precision raster milling, Int. J. Mach. Tools Manuf. 80–81 (2014) 11–17.
[15] S. Wojciechowski, M. Wiackiewicz, G.M. Krolczyk, Study on metrological relations between instant tool displacements and surface roughness during precise ball end milling, Measurement 129 (2018) 686–694.
[16] D. Gao, Z. Liao, Z. Lv, Y. Lu, Multi-scale statistical signal processing of the cutting force in cutting tool condition monitoring, Int. J. Adv. Manuf. Technol. 80 (2015) 1843–1853.
[17] C. Hui, K. Zhang, W. Ning, B. Luo, Q. Meng, A novel six-state the cutting force model for drilling-countersinking machining process of CFRP-Al stacks, Int. J. Adv. Manuf. Technol. 89 (2017) 2063–2076.
[18] V. Pandiyan, W. Caesarendra, T. Tjahjowidodo, H.H. Tan, In-process tool condition monitoring in compliant abrasive belt grinding process using support vector machine and genetic algorithm, J. Manuf. Processes 31 (2018) 199–213.
[19] C. Sohyung, S. Asfour, O. Arzu, Tool breakage detection using support vector machine learning in a milling process, Int. J. Mach. Tools Manuf. 45 (2005) 241–249.
[20] C. Letot, R. Serra, M. Dossevi, P. Dehombreux, Cutting tools reliability and residual life prediction from degradation indicators in turning process, Int. J. Adv. Manuf. Technol. 86 (2016) 495–506.
[21] J.C. Jáuregui, J.R. Reséndiz, S. Thenozhi, T. Szalay, Á. Jacsó, M. Takács, Frequency and time-frequency analysis of the cutting force and vibration signals for tool condition monitoring, IEEE Access 6 (2018) 6400–6410.
[22] J. Dong, K.Y.R. Subrahmanyam, Y.S. Wong, Bayesian-inference-based neural networks for tool wear estimation, Int. J. Adv. Manuf. Technol. 30 (2006) 797–807.
[23] A.I. Azmi, Monitoring of tool wear using measured machining forces and neuro-fuzzy modelling approaches during machining of GFRP composites, Adv. Eng. Softw. 82 (2015) 53–64.
[24] M. Nouri, B.K. Fussell, B.L. Ziniti, E. Linder, Real-time tool wear monitoring in milling using a cutting condition independent method, Int. J. Mach. Tools Manuf. 89 (2015) 1–13.
[25] X.C. Cao, B.Q. Chen, B. Yao, W.P. He, Combining translation-invariant wavelet frames and convolutional neural networks for intelligent tool wear state identification, Comput. Ind. 106 (2019) 71–84.
[26] D.M. D'Addona, A.M.M. Sharif Ullah, D. Matarazzo, Tool-wear prediction and pattern-recognition using artificial neural networks and DNA-based computing, J. Intell. Manuf. 28 (2017) 1285–1301.
[27] R. Corne, C. Nath, M.E.I. Mansori, T. Kurfess, Study of spindle power data with neural networks for predicting real-time tool wear/breakage during inconel drilling, J. Manuf. Syst. 43 (2017) 287–295.
[28] C. Drouillet, J. Karandikar, C. Nath, A.C. Journeaux, M.E.I. Mansori, T. Kurfess, Tool life predictions in milling using spindle power with the neural networks technique, J. Manuf. Processes 22 (2016) 161–168.
[29] P.B. Huang, C.C. Ma, C.H. Kuo, A PNN self-learning tool breakage detection system in end milling operations, Appl. Soft Comput. 37 (2015) 114–124.
[30] G. Xu, Z.H. Zhou, J. Chen, CNC internal data based incremental cost-sensitive support vector machine method for tool breakage monitoring in end milling, Eng. Appl. Artif. Intell. 74 (2018) 90–103.
[31] D. Shi, N.N. Gindy, Tool wear predictive model based on least squares support vector machines, Mech. Syst. Sig. Process. 21 (2007) 1799–1814.
[32] J. Yu, S. Liang, D. Tang, H. Liu, A weighted hidden Markov model approach for continuous-state tool wear monitoring and tool life prediction, Int. J. Adv. Manuf. Technol. 91 (2017) 201–211.
[33] F.A. Niaki, M. Michel, L. Mears, State of health monitoring in machining: extended Kalman filter for tool wear assessment in turning of IN718 hard-to-machine alloy, J. Manuf. Process. 24 (2016) 361–369.
[34] J. Zhang, B. Starly, Y. Cai, P.H. Cohen, Y.S. Lee, Particle learning in online tool wear diagnosis and prognosis, J. Manuf. Process. 28 (2017) 457–463.
[35] F. Penedo, R.E. Haber, A. Gajate, R. M.del Toro, Hybrid incremental modeling based on least squares and fuzzy and *K*-NN for monitoring tool wear in turning processes, IEEE Trans. Ind. Inf. 8 (2012) 811–818.